Coordination Chemistry of Verdazyl Radicals: Group 12 Metal (Zn, Cd, Hg) Complexes of 1,4,5,6-Tetrahydro-2,4-dimethyl-6-(2′-pyridyl)-1,2,4,5-tetrazin-3(2*H*)-one ($pvdH_3$) and 1,5-Dimethyl-3-(2′-pyridyl)-6-oxoverdazyl (pvd)

David J. R. Brook,*,† Spring Fornell,† Jonathan E. Stevens,† Bruce Noll,‡ Tad H. Koch,‡ and Wolfgang Eisfeld§

University of Detroit Mercy, P.O. Box 19900, Detroit, Michigan 48219-0900, University of Colorado, Boulder, Colorado 80309-0215, and Cherry L. Emerson Center for Scientific Computation and Department of Chemistry, Emory University, Atlanta, Georgia 30322

Received April 8, 1999

Ferricyanide oxidation of 1,4,5,6-tetrahydro-2,4-dimethyl-6-(2′-pyridyl)-1,2,4,5-tetrazin-3(2*H*)-one ($pvdH_3$) produces the stable chelating free radical 1,5-dimethyl-3-(2′-pyridyl)-6-oxoverdazyl (pvd) as an orange solid. Combination of group 12 metal halides with the ligand $pvdH_3$ in acetonitrile results in precipitation of metal complexes. The mercuric chloride complex crystallizes in the monoclinic space group $P2_1/c$ with unit cell dimensions $a = 8.5768(8)$ Å, $b = 19.1718(17)$ Å, $c = 8.5956(8)$ Å, $\beta = 90.405°$, and $V = 1413.4(2)$ Å^3. The mercuric ion is tricoordinate with a distorted trigonal planar geometry. Cadmium iodide and zinc chloride induce ring opening of the tetrazine resulting in pentacoordinate complexes of a hydrazone ligand. The cadmium iodide complex crystallizes in the triclinic space group $P\bar{1}$ with cell dimensions $a = 7.7184(8)$ Å, $b = 8.0240(9)$ Å, $c = 13.348(2)$ Å, $\alpha = 97.876(4)°$, $\beta = 95.594(6)°$, $\gamma = 107.304(6)°$, and $V = 773.40(21)$ Å^3. Oxidation of all three metal complexes produces verdazyl radicals. Metal coordination is indicated by small changes in the EPR spectrum and by changes in the UV−visible spectrum, in particular the changes in the position of bands in the visible region. The metal halide−pvd complexes can also be synthesized by direct combination of metal halides with the free radical.

Introduction

Interest in the metal complexes of stable free radicals stems from their potential as building blocks for the formation of molecular magnetic materials.[1] In addition, there is great potential for open-shell ligands as a means to modify the electronic structure of self-assembled coordination arrays such as those described by Lehn.[2] Such modified arrays may be useful in the construction of molecular devices. The increasing variety of stable radical ligands reported[3] provides a broad base for the synthesis of many interesting complexes and materials; however, to fully utilize stable free radicals as ligands it is important to understand the nature of the metal−ligand interaction. Recent publications describing the coordination chemistry of the 1,1′,5,5′-tetramethyl-6,6′-dioxo-3,3′-biverdazyl (bvd) diradical suggest that there is significant orbital overlap between the d^{10} metal center Cu(I) and the diradical ligand. This interaction gives rise to an unusually rapid spin−lattice relaxation rate and a strong ferromagnetic exchange pathway between the free radical ligands.[4] We are seeking to further characterize the metal−verdazyl interaction through the synthesis of other chelating verdazyls and the characterization of their metal complexes. The group 12 dications (Zn^{2+}, Cd^{2+}, and Hg^{2+}), like copper(I), have filled d orbitals, but unlike Cu(I) they are far less prone to oxidation and charge transfer and are relatively weak π donors. Despite this, earlier studies with triphenylverdazyl showed irreversible formation of diamagnetic products with these metals.[5,6] We seek to investigate the coordination chemistry of the group 12 metals with oxoverdazyls as part of a more general study of oxoverdazyl coordination chemistry. Free radical ligands with one chelation site are more likely than bridging ligands (such as bvd) to form discrete, soluble complexes that are more amenable to study. We report the synthesis of the chelating verdazyl radical 1,5-dimethyl-3-(2′-pyridyl)-6-oxoverdazyl (pvd) and the characterization of its complexes with zinc, cadmium, and mercury by EPR and UV−vis spectroscopy. We also report the formation of these complexes through oxidation of the corresponding complexes of the free radical precursor 1,4,5,6-tetrahydro-2,4-dimethyl-6-(2′-pyridyl)-1,2,4,5-tetrazin-3(2*H*)-one ($pvdH_3$).

Experimental Section

General Methods. 1,1′-Dimethyl carbonic dihydrazide was synthesized from phosgene and methylhydrazine as described by Neugebauer.[7] Tetraphenylhydrazine was synthesized by oxidation of diphenylamine with potassium permanganate in acetone as described by Gatterman and Wieland.[8] NMR spectra were acquired with Varian Unity 500 500

† University of Detroit Mercy.
‡ University of Colorado.
§ Emory University.

(1) Kahn, O. *Molecular Magnetism*; VCH: New York, 1993.
(2) Lehn, J. M. *Supramolecular Chemistry*; VCH: Weinheim, Germany, 1995.
(3) Shultz, D. A.; Boal, A. K.; Farmer, G. T. *J. Org. Chem.* **1998**, *63*, 9462.
(4) Brook, D. J. R.; Conklin, B.; Lynch, V.; Fox, M. A. *J. Am. Chem. Soc.* **1997**, *119*, 5155.
(5) Degtyarev, L. S.; Maletin, Y. A.; Stetsenko, A. A. *Zh. Obshch. Khim.* **1981**, *51*, 2387.
(6) Strizhakova, N. G.; Maletin, Y. A.; Sheka, I. A. *Zh. Obshch. Khim.* **1983**, *53*, 498.
(7) Neugebauer, F. A.; Fischer, H.; Siegel, R.; Kreiger, C. *Chem. Ber.* **1983**, *116*, 3461.
(8) Gatterman, L.; Wieland, T. *Die Praxis Des Organischen Chemikers*; W. de Gruyter: Berlin, 1956.

10.1021/ic9903883 CCC: $19.00
Published on Web 01/19/2000

MHz or VXR 300S 300 MHz spectrometers Chemical shifts were referenced to the residual proton signal of the solvent. IR spectra were recorded on a Perkin-Elmer Spectrum 2000 FTIR spectrometer by diffuse reflectance from a KBr dispersion. UV−visible spectra were recorded on a Hewlett-Packard 8452 diode array spectrophotometer. Mass spectra were recorded on a VG-7070 EQ-HF hybrid tandem mass spectrometer. EPR spectra were recorded on a Bruker ESP-300e spectrometer.

1,4,5,6-Tetrahydro-2,4-dimethyl-6-(2′-pyridyl)-1,2,4,5-tetrazin-3(2*H*)-one (pvdH$_3$). 1,1′-Dimethyl carbonic dihydrazide (1.18 g, 10 mmol) was dissolved in absolute methanol and a solution of pyridine-2-carboxaldehyde (1.07 g, 10 mmol) in methanol added dropwise with stirring at room temperature. After addition was complete, the solution was stirred for 10 min and evaporated to give 1.88 g (90%) of the crude product as a sticky yellow crystalline solid. A pure sample was obtained by chromatography on silica gel eluting with ethyl acetate, followed by recrystallization from a small amount of methanol; the product crystallized as large colorless blocks with mp 154−156 °C: ^{1}H NMR(CDCl$_3$) δ 3.126 (s, 6H), 4.84 (bs, 1H), 5.4 (v broad singlet, 2H, NH), 7.27 (ddd, 1H, $J_1 = 1.2$ Hz, $J_2 = 5.0$ Hz, $J_3 = 7.5$ Hz), 7.42 (dt, 1H, $J_1 = 7.5$ Hz, $J_2 = J_3 = 1.2$ Hz), 7.71 (td, 1H, $J_1 = J_2 = 7.5$ Hz, $J_3 = 1.5$ Hz), 8.515 (ddd, 1H, $J_1 = 5.0$ Hz, $J_2 = 1.5$ Hz, $J_3 = 1.2$ Hz); ^{13}C NMR (CDCl$_3$) δ 38.0, 69.4, 123.5, 124.2, 137.2, 149.5, 153.5, 154.5; IR (KBr) 3244 (NH), 3187 (NH), 3051, 2925, 1631(C═O), 1598, 1482, 1443, 1381, 1118, 1099, 1000, 948, 870, 782, 754, 730, 670, 642, 620, 604; MS (EI, 70 eV) *m*/*z* (rel intensity) 207 (9, M$^+$), 162 (95), 79 (79), 78 (70), 71 (100), 45 (55) 31 (90), 28 (88). Anal. Calcd for $C_9H_{13}N_5O$: C, 52.16; H, 6.32; N, 33.79. Found: C, 52.08; H, 6.19; N, 33.76.

Complexes of pvdH$_3$ with Group 12 Metal Halides. pvdH$_3$ (0.1 mmol) was dissolved in 1 mL of acetonitrile. This solution was combined with a solution of 0.1 mmol of metal halide in 1 mL of acetonitrile and the solution allowed to stand overnight. Colorless crystals were deposited over a 15 h period.

$ZnCl_2$ (13.6 mg) and pvdH$_3$ (20 mg) gave 23.8 mg (70%) of $ZnCl_2$(py-hydrazone) as a microcrystalline powder. In DMSO-d_6 ^{1}H NMR signals were observed for a hydrazone complex, δ 8.58 (m, 1H), 7.94 (m, 1H), 7.85 (m, 2H) (overlapping signals from pyridyl H and imine H), 7.43 (m, 1H), 5.31 (bs, 2H), 3.32 (s, 3H), and 3.14 (s, 3H), and for the uncomplexed ligand, δ 8.55 (1H, m), 7.84 (1H, m), 7.54 (1H, m), 7.39 (1H, ddd), 5.61 (2H, d), 4.90 (1H, t), and 2.95 (6H, s). After 30 min, only signals for the uncomplexed ligand were observed. IR (KBr): 3315, 3049, 1670 (C═O), 1620 (C═N), 1596, 1486, 1463, 1278, 1207, 1115, 1054, 925, 777, 747, 407. Anal. Calcd for $C_9H_{13}Cl_2N_5OZn$: C, 31.54; H, 3.79; N, 20.44. Found: C, 31.90; H, 3.85; N, 20.20.

CdI_2 (70 mg) and 40 mg of pvdH$_3$ gave 46 mg (42%) of CdI_2(py-hydrazone) as colorless blades. In DMSO-d_6 ^{1}H NMR signals were observed for a hydrazone complex, δ 3.127 (s, 3H), 3.294 (s, 3H), and 5.029 (bs, 2H), and aromatic proton chemical shifts were determined by comparison with an authentic sample of pvdH$_3$ in DMSO, δ 7.4 (m, 1H), 7.85 (m, 2H), and 8.55 (d, 1H). Signals were also observed for the uncomplexed ligand. After 30 min, only the latter signals remained. IR (KBr): 3303 (N−H), 1667 (C═O), 1593 (C═N), 1485, 1465, 1393, 1371, 1307, 1274, 1203, 1043, 917, 778, 742, 690, 640, 603, 517, 405. Anal. Calcd for $C_9H_{13}CdI_2N_5O$: C, 18.86; H, 2.27; N, 12.22. Found: C, 19.25; H, 2.23; N, 12.02.

$HgCl_2$ (61 mg) and 46 mg of pvdH$_3$ gave 56 mg (52%) of $HgCl_2$(pvdH$_3$) as colorless blocks. In DMSO-d_6 ^{1}H NMR gave signals only for the uncomplexed ligand. IR (KBr): 3234 (N−H), 3143 (C−H), 2923 (C−H), 1626 (C═O), 1507, 1441, 1398, 1352, 1321, 1302, 1217, 1101, 1056, 1015, 980, 876, 783, 723, 633, 530, 476, 409. Anal. Calcd for $C_9H_{13}Cl_2HgN_5O$: C, 22.64; H, 2.73; N, 14.68. Found: C, 22.78; H, 2.68; N, 14.69.

Crystallography. Crystals were examined under light hydrocarbon oil and mounted to a thin glass fiber attached to a tapered copper mounting-pin using a small amount of silicone grease. After optical alignment of the specimen in the 3-circle goniometer of a Siemens SMART CCD equipped with a LT-2A low-temperature apparatus, a series of 3 orthogonal sets of 20 0.3° ω scans was measured to determine crystal quality and preliminary cell dimensions. Actual data collection covered an arbitrary volume of space, a hemisphere for the Hg complex and a full sphere for the Cd complex. Data frames were also 0.3° ω scans, each exposed for a total of 30 s using 2 correlated 15 s scans. Data were integrated with SAINT,[9] and cell parameters were refined using reflections with $I > 10\sigma(I)$ harvested from the complete data set. All data were corrected for Lorentz and polarization effects as well as for absorption.

Initial phasing was determined by direct methods, which revealed most of the non-hydrogen atoms. Cycles of least-squares refinement followed by difference Fourier synthesis located any missing atoms. Hydrogens were placed at calculated positions and released to refine in later cycles of least squares. Non-hydrogen atoms were refined with anisotropic parameters for thermal motion; hydrogens utilized isotropic parameters for thermal motion. Residual electron density peaks were located near heavy atoms and likely result from absorption. Solution, refinement and molecular graphics used the SHELXTL[10] package of crystallographic software and the graphics program ORTEX.[11] Full details of these structure determinations can be found in the Supporting Information.

1,5-Dimethyl-3-(2′-pyridyl)-6-oxoverdazyl (pvd). pvdH$_3$ (103.8 mg, 0.5 mmol) was dissolved in 1 mL of water. Potassium ferricyanide (498 mg, 1.5 mmol) was combined with 10 drops of 2 M Na_2CO_3(aq) and 2 mL of water. When dissolution was complete, the two solutions were combined. Vigorous effervescence ensued, and the solution turned dark. After ∼30 s an orange-red precipitate of the 1,5-dimethyl-3-(2′-pyridyl)-6-oxoverdazyl formed. This was removed by filtration, washed with cold saturated aqueous NaCl, and dried. The orange-red solid weighed 53.8 mg. IR (KBr): 1686 (C═O), 1585, 1473, 1440, 1373, 1296, 1252, 1210, 1146, 1093, 1050, 998, 793, 744 cm^{-1}. Contamination with ferrocyanide was revealed by a peak at 2040 cm^{-1}. MS (EI, 70 eV) [*m*/*z* (relative intensity)]: 205 (M + 1, 93), 191 (44), 177 (11), 134 (15), 105 (100). HPLC (cyanoalkyl-derivatized 200 mm silica gel column, flow rate 0.5 mL/min, 5 min isocratic elution with pH 7.4 triethylammonium acetate buffer followed by a 15 min gradient to 80% acetonitrile) confirmed that this solid contained only two UV absorbing components. The first, eluting at 5.1 min, was identified as ferrocyanide by co-injection with an authentic sample. The second component, eluting at 20.2 min, had a UV spectrum very similar to that of the previously reported 1,5-dimethyl-3-phenyl-6-oxoverdazyl. The solid material was partially soluble in acetonitrile, and the resulting solutions, after filtration, had UV spectra identical to those obtained by HPLC. Extinction coeficients were estimated using the mass of dissolved sample. EPR spectroscopy in benzene gave a spectrum indistinguishable from that obtained upon oxidation with tetraphenylhydrazine (vide infra).

Oxidation of pvdH$_3$ and Metal pvdH$_3$ Complexes with Tetraphenylhydrazine. pvdH$_3$ (2 mg, 0.01 mmol) and tetraphenylhydrazine (5 mg, 0.015 mmol) were combined in 2 mL of benzene in an EPR tube. The mixture was freeze−pump−thaw degassed (3 cycles) and heated at 80 °C for 4 h. EPR spectroscopy gave a spectrum indistinguishable from that obtained by simulation with the hyperfine coupling published for 1,5-dimethyl-3-phenyl-6-oxoverdazyl.[12] Similarly, in a representative reaction, $HgCl_2$(pvdH$_3$) (3.4 mg) was combined with tetraphenylhydrazine (2.49 mg) in 2 mL of benzene in an EPR tube. The sample was freeze−pump−thaw degassed for three cycles and sealed under vacuum. The sample was heated at ∼80 °C for 4 h during which time a pale yellow color developed and an EPR signal appeared. Spectral parameters are summarized in Table 5.

Results

The free radical precursor 1,4,5,6-tetrahydro-2,4-dimethyl-6-(2′-pyridyl)-1,2,4,5-tetrazin-3(2*H*)-one (pvdH$_3$) was readily synthesized by condensation of 1,1′-dimethyl carbonic dihydrazide with pyridine-2-carboxaldehyde in ethanol (Scheme 1). The product was isolated as colorless blocky crystals.

(9) *SAINT v. 4.050*; Siemens: Madison, WI, 1995.
(10) Sheldrick, G. M. *SHELXTL, A Program for Crystal Structure Determination v. 5.03*; Madison, WI, 1995.
(11) McArdle, P. *J. Appl. Crystallogr.* **1995**, *28*, 65.
(12) Neugebauer, F. A.; Fischer, H.; Siegel, R. *Chem. Ber.* **1988**, *121*, 815.

Scheme 1

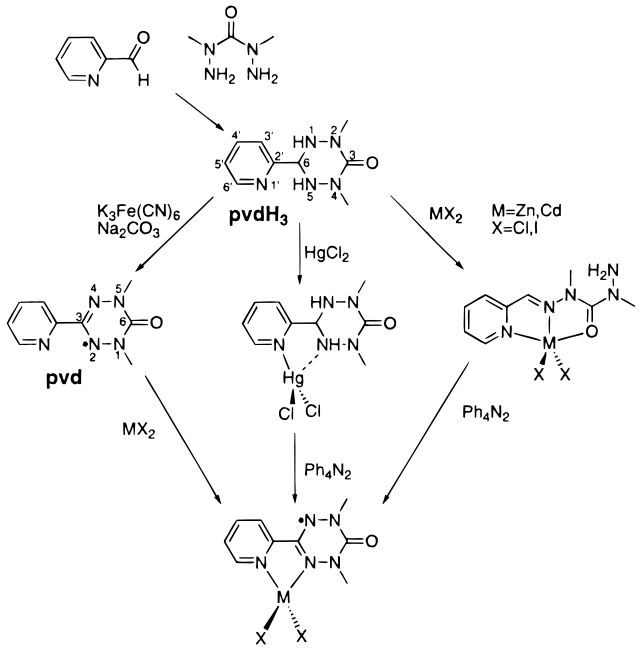

Oxidation of a benzene solution of $pvdH_3$ with tetraphenylhydrazine under vacuum generated a solution containing 1,5-dimethyl-3-(2′-pyridyl)-6-oxoverdazyl (pvd) as indicated by EPR. The EPR spectrum in benzene was indistinguishable from that reported for 1,5-dimethyl-3-phenyl-6-oxoverdazyl[12] with coupling to all four verdazyl nitrogens and the six methyl hydrogens. No coupling was observed to either the hydrogens or nitrogen of the pyridine ring. Simulated and experimental spectra are shown in Figure 1. Though partly obscured by the presence of diphenylamine, the UV−visible spectrum of this solution reveals long-wavelength bands at 408 and 450 nm due to the free radical. Oxidation of a saturated solution of $pvdH_3$ in water with ferricyanide produced an orange solid also containing 1,5-dimethyl-3-(2′-pyridyl)-6-oxoverdazyl as indicated by EPR. Reverse-phase HPLC with diode array detection indicates that this solid contains ferrocyanide and 1,5-dimethyl-3-(2′-pyridyl)-6-oxoverdazyl radical, identified by its UV−visible spectrum which is comparable to that of an authentic sample of the previously characterized 1,5-dimethyl-3-phenyl-6-oxoverdazyl. UV−visible spectra of pvd and the metal complexes of pvd (vide infra) are shown in Figure 2. Solid samples and solutions of pvd decompose slowly in air, producing several different products (observed by HPLC) which were not characterized. Because of this instability, a pure sample of pvd was not obtained.

Combination of $pvdH_3$ with 1 molar equiv of each of the group 12 metal halides $HgCl_2$, CdI_2, and $ZnCl_2$, resulted in the formation of crystalline precipitates of the $pvdH_3$ metal complexes. The $HgCl_2$ and CdI_2 complexes were characterized by X-ray crystallography; the $ZnCl_2$ complex did not form crystals of sufficient quality and was characterized by spectroscopic techniques alone. Unit cell data and details of data collection, solution, and refinement are summarized in Table 1. The structure of $HgCl_2(pvdH_3)$ is depicted in Figure 3. The tetrazine ring is puckered, with nitrogen atoms at the 2 and 4 positions and the carbon atom at the 3 position showing the expected sp^3-hybridized geometry. The mercury atom is coordinated to the pyrazine nitrogen and shows a distorted trigonal planar geometry. A summary of significant distances and bond lengths and angles is given in Table 2. Though the N(1) (crystallographic numbering) lone pair is directed toward the mercury atom, the Hg−N(1) distance (2.57 Å) is longer than an Hg−N single bond but well within the van der Waals distance. The weak nature of the interaction is demonstrated in the NMR spectrum of the complex in DMSO. Though the proton chemical shifts, particularly those of the amine hydrogens, differ from those of the free ligand, the resonances from the tetrazine ring are symmetric indicating that the mercury atom can only be coordinated to the pyridine ring. The coordination products with CdI_2 and $ZnCl_2$ differ significantly from that with $HgCl_2$. Cadmium(II) is sufficiently Lewis acidic to induce ring opening of the tetrazine ring producing the hydrazone ligand 1′-methyl-2′-(2″-pyridylmethylene)-hydrazino-1-methyl carbonic hydrazide (py-hydrazone). In the resulting complex cadmium is pentacoordinate with a distorted trigonal bipyramidal geometry, coordinated to the pyridine nitrogen, imine nitrogen, and carbonyl oxygen of the hydrazone ligand (Figure 3). The cadmium, both iodide anions, and the equatorial imine nitrogen are approximately coplanar, but the bond angles are significantly

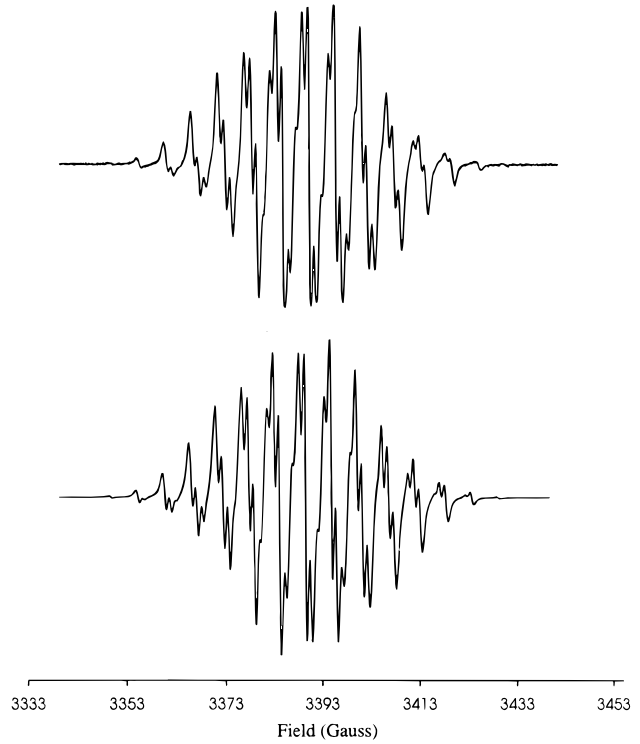

Figure 1. Experimental (top) and simulated (bottom) EPR spectra for pvd. Coupling constants are identical to those reported by Neugebauer: $a_{N1,5} = 5.2$; $a_{N2,4} = 6.4$; $a_H = 5.4$; $g = 2.0036$.

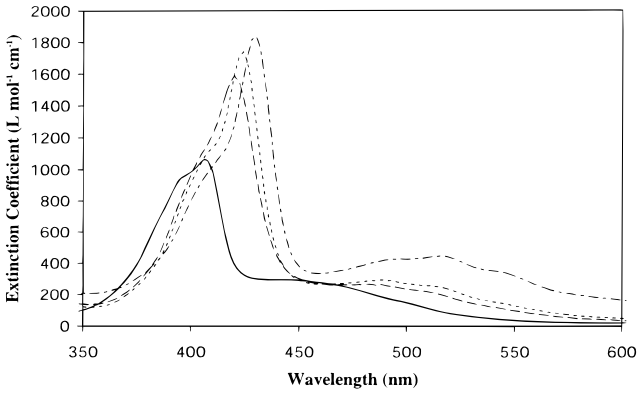

Figure 2. Visible spectra for pvd (—), $HgCl_2$(pvd) (— — —), CdI_2-(pvd) (- - -), and $ZnCl_2$(pvd) (— - —).

Table 1. Data Collection Parameters for $HgCl_2(pvdH_3)$ and CdI_2(py-hydrazone)

compd	$HgCl_2(pvdH_3)$	CdI_2(py-hydrazone)
empirical formula	$C_9H_{13}Cl_2HgN_5O$	$C_9H_{13}CdI_2N_5O$
fw	478.73	573.44
cryst syst	monoclinic	triclinic
space group	$P2_1/c$	$P\bar{1}$
a (Å)	8.5768(8)	7.7184(8)
b (Å)	19.1718(17)	8.0240(9)
c (Å)	8.5956(8)	13.348(2)
α (deg)	90	97.876(4)
β (deg)	90.405(5)	95.594(6)
γ (deg)	90	107.304(6)
V (Å^3)	1413.4(2)	773.40(21)
Z	4	2
ρ_{calc} (g·cm^{-3})	2.250	2.462
μ (mm^{-1})	11.263	5.400
transm coeff	0.2659 and 0.1907	0.46 and 0.89
T (K)	156(2)	161(2)
λ, Å	0.710 73 (Mo Kα)	0.710 73 (Mo Kα)
reflcns collcd	12817	10098
unique reflcns	4272 (R(int) = 0.0247)	4518 (R(int) = 0.0380)
reflcns obsd	3869	3787
R index[a] [$I > 2\sigma(I)$]	R1 = 0.0236	R1 = 0.0335
R indices[a] (all data)	R1 = 0.0284, wR2 = 0.0506	R1 = 0.0412, wR2 = 0.0832
weighting coeffs[b]	$a = 0.0136$, $b = 2.2363$	$a = 0.0426$, $b = 0.0426$
goodness-of-fit[c] on F^2	1.126	0.970

[a] $R1 = (\sum||F_o| - |F_c||)/\sum|F_o|$; $wR2 = \{(\sum[w(F_o^2 - F_c^2)])/(\sum[w(F_o^2)])\}^{1/2}$. [b] $w^{-1} = [\sigma^2(F_o^2) + (aP)^2 + bP]$, where $P = (F_o^2 + 2F_c^2)/3$. [c] $GOF = S = \{(\sum[w(F_o^2 - F_c^2)^2])/(M - N)\}^{1/2}$, where M is the number of reflections and N is the number of parameters refined.

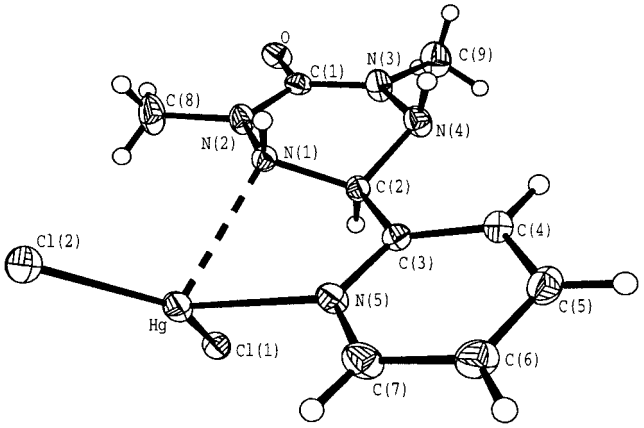

Figure 3. Thermal ellipsoid plot of $HgCl_2(pvdH_3)$. Ellipsoids are plotted at the 50% probability level.

Table 2. Selected Distances and Angles for $HgCl_2(pvdH_3)$

dist (Å)		angle (deg)	
Hg−Cl(1)	2.4124(8)	Cl(1)−Hg−Cl(2)	141.24(3)
Hg−Cl(2)	2.3607(8)	N(5)−Hg−Cl(1)	107.20(6)
Hg−N(2)	2.59	N(5)−Hg−Cl(2)	111.56(7)
Hg−N(5)	2.371(3)	C(3)−N(5)−Hg(1)	118.52(19)
N(2)−N(1)	1.430(3)	C(7)−N(5)−Hg(1)	122.3(2)
N(1)−C(2)	1.471(4)	N(2)−Hg−Cl(2)	102.82
		N(2)−Hg−Cl(1)	91.92

different from the ideal 120°. The pyridine nitrogen and carbonyl oxygen also deviate from the ideal 90° angle from the equatorial plane, presumably because of the small bite angle of the ligand. Bond lengths and angles are given in Table 3. Spectroscopic evidence (NMR and IR) suggests that the zinc complex has a structure analogous to the cadmium complex. The Zn and Cd complexes are labile in solution as evidenced by the ^{1}H NMR spectra in DMSO-d_6. Shortly after dissolution in DMSO the $ZnCl_2$ and CdI_2 complexes give ^{1}H NMR spectra with signals from both the $pvdH_3$ and py-hydrazone ligands. Differences in chemical shift between the cadmium and zinc complexes suggest that the py-hydrazone ligand is still coordinated to the metal. After 30 min only signals corresponding to the free ligand $pvdH_3$ are observed suggesting that dissociation of the metal is accompanied by cyclization. NMR data for $pvdH_3$ and its Zn, Cd, and Hg complexes in DMSO are summarized in Table 4.

Table 3. Selected Bond Lengths and Angles for CdI_2(py-hydrazone)

dist (Å)		angle (deg)	
Cd−I(1)	2.7389(4)	I(1)−Cd−I(2)	112.210(12)
Cd−I(2)	2.7342(4)	I(1)−Cd−N(2)	108.83(7)
Cd−N(2)	2.364(3)	I(2)−Cd−N(2)	138.93(7)
Cd−N(5)	2.351(3)	N(2)−Cd−O	65.67(10)
Cd−O	2.388(3)	N(2)−Cd−N(5)	69.24(11)
C(2)−N(2)	1.291(5)	O−Cd−I(1)	104.59(7)
N(1)−N(2)	1.372(4)	O−Cd−I(2)	101.63(7)
N(1)−C(1)	1.400(5)	I(1)−Cd−N(5)	104.10(8)
C(1)−O	1.242(5)	I(2)−Cd−N(5)	101.81(8)
C(1)−N(4)	1.347(5)	O−Cd−N(5)	132.20(10)

Oxidation of $pvdH_3$−metal complexes with tetraphenylhydrazine under vacuum, or combination of acetonitrile solutions of the crude pvd and metal halides, gave solutions containing metal-coordinated pvd radicals which were characterized by UV−visible and EPR spectroscopy.

Evidence for metal coordination to the pvd radical was obtained from the UV−visible spectra. Acetonitrile solutions containing metal halides and pvd were analyzed by reverse phase HPLC eluting with acetonitrile and the spectra recorded with diode array detection. In addition, varying concentrations of metal halides were added to acetonitrile solutions of pvd and the spectral changes monitored. Coordination results in a shift of the two low-energy bands to longer wavelength combined with an increase in intensity. Electronic spectra in the visible region are plotted in Figure 2. The effect is more pronounced for Zn than Hg with Cd lying in between. For zinc and cadmium, addition of excess halide does not change the spectrum indicating that the metal is relatively strongly bound. For mercury, the binding is significantly weaker, the spectrum in Figure 2 being obtained with a large excess of $HgCl_2$. By measurement of the spectrum at intermediate concentrations we estimate the equilibrium constant for the reaction

$$\text{pvd} + HgCl_2 \rightleftharpoons HgCl_2(\text{pvd})$$

as 6×10^2 L mol^{-1}. The spectral changes result in a distinct change in color of the free radical solution from yellow-orange to orange-red upon addition of metal halides. Despite the clear evidence for metal coordination, only small changes were observed in the EPR spectra. Data for the EPR spectra are given in Table 5. Unfortunately, evaporation of these solutions did not give clean samples of the metal pvd complexes.

To supplement our understanding of these spectral changes, molecular orbital calculations were performed on the pvd molecule to identify the nature of the two lowest energy transitions. All calculations described here were performed with the GAUSSIAN 98[13] electronic structure package. The geometry of the radical was optimized with the AM1 semiempirical method. The resulting structure is rather distorted from C_s symmetry. The torsional angle between the two planar rings,

(13) Frisch, M. J.; et al. *Gaussian 98 A*, revision A6; Gaussian, Inc.: Pittsburgh, PA, 1998.

Table 4. NMR Resonances for $pvdH_3$ and $pvdH_3$ Metal Complexes in DMSO Solution

	group						
	$-CH_3$	NH($pvdH_3$) or NH_2(py-hydrazone)	CH	C^3H	C^4H	C^5H	C^6H
$pvdH_3$ (DMSO)	2.95, s	5.61, d	4.90, t	7.54, d	7.83, td	7.39, dd	8.55, d
$pvdH_3$/Cd	2.95, s	5.64, d	4.92, t	7.55, d	~7.84, td	~7.40, dd	8.54, d
$pvdH_3$/Zn	2.95, s	5.61, d	4.90, t	7.54, d	7.84, td	7.39, dd	8.55, d
$pvdH_3$/Hg	2.96, s	5.76, d	4.97, t	7.59, d	7.89, td	7.44, dd	8.58, d
hydrazone/Zn	3.14, s; 3.32, bs	5.31, bs	7.85, bs	7.94, d	7.85, m	7.43, dd	8.58, d
hydrazone/Cd	3.13, s; 3.29, bs	5.03, bs	7.76, bs	~7.88, m	~7.85, m	~7.4, dd	8.57, d

Table 5. EPR Spectral Data for pvd and Its Metal Complexes with Hyperfine Coupling Constants Reported in G

	g	$a_N(1,5)$	$a_N(2,4)$	a_H
pvd	2.0035	5.2	6.5	5.5
$ZnCl_2$(pvd)	2.0054	6.2	6.2	6.2
CdI_2(pvd)	2.0056	5.7	5.7	5.8
$HgCl_2$(pvd)	2.0079	5.6	6.8	5.6

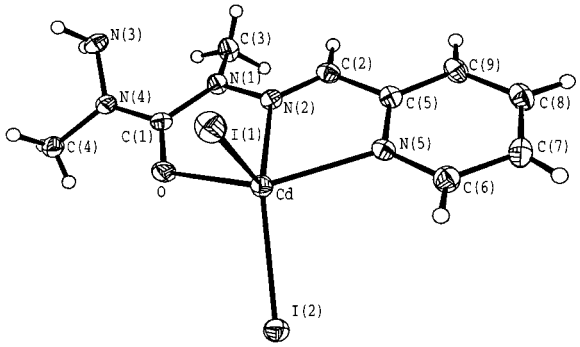

Figure 4. Thermal ellipsoid plot of CdI_2(py-hydrazone). Ellipsoids are plotted at the 50% probability level.

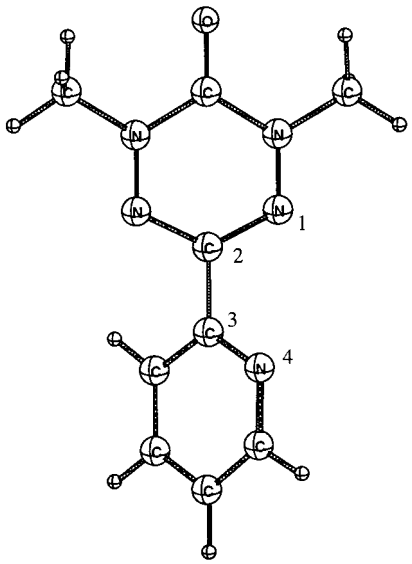

Figure 5. Structure of the pvd radical as optimized by the AM1 semiempirical method. The N1−C2−C3−N4 dihedral angle is 49.5°.

as defined by the N−C−C−N dihedral angle (Figure 5), is 49.5°. A configuration interaction singles (CIS) calculation implementing a 6-31+G(d) basis and an unrestricted Hartree−Fock reference function was then performed at the optimized geometry to characterize the states accessed upon UV excitation. To a first approximation, the two lowest transitions can be characterized as HOMO−SOMO ($n\rightarrow\pi$) and SOMO−LUMO ($\pi\rightarrow\pi^*$), respectively, though there is significant mixing between the two. The lowest energy transition ($n\rightarrow\pi$) is calculated to be at 366 nm (3.38 eV) and is dark, with a transition moment of 0.015 au. The higher energy transition ($\pi\rightarrow\pi^*$) is calculated to be at 303 nm (4.09 eV) with a transition moment of 0.262 au. The vertical excitation energies differ strikingly from the experimental UV absorption band maxima, which appear around 450 and 408 nm for the first and second transitions, respectively. The calculation does qualitatively reproduce the relative brightness of the two low-lying states. The difference in computed and experimental excitation energies may result from solvation effects in the experiment, which are not treated in the calculation. The optimized geometry may also account for the deviation of theory and experiment; recent studies[14,15] of the similar 1,1′5,5′-tetramethyl-6,6′-dioxo-3,3′-biverdazyl diradical (bvd) find that geometry optimizations at lower levels of theory (AM1, ROHF) produce nonzero torsional angles while optimizations using the hybrid density functional B3LYP method produce zero or near-zero torsion angles.[14]

Discussion

Neugebauer and co-workers reported a wide variety of 6-oxoverdazyl radicals in their initial publications,[12,16] so the straightforward synthesis of $pvdH_3$ and pvd is not surprising. The ring opening of the tetrazine to a hydrazone is unexpected but might be anticipated from the Lewis acidity of the metal centers. Certainly the weakest Lewis acid (Hg^{2+}) does not induce ring opening and the large Cl−Hg−Cl angle (141°) suggests that coordination to mercury is relatively weak. The cadmium and zinc complexes are similar to the pentacoordinate zinc complex reported by Zakrzewski and co-workers.[17] All three complexes are relatively labile in DMSO. Though NMR spectra of the Zn^{2+} and Cd^{2+} complexes were observed, the species decompose within 30 min, ligand substitution being accompanied by reclosure of the tetrazine ring. Somewhat surprisingly there was no NMR evidence for a Zn^{2+} or Cd^{2+} coordinated to the ring-closed ligand in DMSO solution. In acetonitrile, where complex formation is favored, oxidation of the metal complex results in reclosure of the ring to form a verdazyl radical.

The unpaired electron of the 6-oxoverdazyl radical is located in a formally antibonding molecular orbital localized largely on the four nitrogen atoms, as shown by the ab initio calculations. This result is similar to that obtained in computational studies of the 1,5-dimethyl-3-phenyl-6-oxoverdazyl radical by Barone et al.[14] Coordination of the group 12 metals to pyridyl verdazyls results in only small changes unpaired electron distribution as shown by the EPR spectra. This contrasts with the triphenylverdazyl radical which undergoes electron-transfer reactions with Lewis acids such as $TiCl_4$, $AlCl_3$, and BF_3[18] and also reduces mercuric chloride to mercurous chloride and

(14) Barone, V.; Bencini, A.; Ciofini, I.; Daul, C. *J. Phys. Chem. A* **1999**, *103*, 4275.
(15) Green, M. T.; McCormick, A. T. *Inorg. Chem.* **1999**, *38*, 3061.
(16) Neugebauer, F. A.; Fischer, H. *Angew. Chem., Int. Ed. Engl.* **1980**, *92*, 761.
(17) Zakrzewski, G.; Lingafelter, E. C. *Inorg. Chim. Acta* **1970**, *4*,

metallic mercury.[19] Zinc and cadmium are reported to induce disproportionation of triphenylverdazyl radical,[5,6] but we have seen no evidence for disproportionation in our experiments. Introduction of the carbonyl group into the verdazyl ring probably results in a significant reduction in SOMO orbital energy and stabilizes the radical toward disproportionation, possibly through the captodative effect.[20,21] Changes in the UV−visible spectra confirm that there is some interaction between metal ions and the free radical π system but also indicate that, at least for mercury, the metal binding is relatively weak. This is similar to the weak ligand perturbation observed in other polypyridyl complexes of Zn and Cd[22] and contrasts with the observation of strong metal−ligand charge transfer (MLCT) bands in the copper complexes of the bis(verdazyl) diradical.[4] In this respect the verdazyl ligand seems to have similar properties to other polypyridyl ligands and we anticipate that the coordination chemistry of polypyridyl ligands will provide a solid foundation for the understanding of verdazyl coordination chemistry.

(18) Dvorko, G. F.; Degtyarev, L. S.; Tomaschik, A. K. *Dokl. Acad. Nauk SSSR* **1972**, *202*, 1073.
(19) Dvorko, G. F.; Degtyarev, L. S. *Zh. Org. Khim.* **1974**, *10*, 1554.
(20) Katritzky, A. R.; Zerner, M. C.; Karelson, M. M. *J. Am. Chem. Soc.* **1986**, *108*, 7213.
(21) Veihe, H. G.; Janousek, Z.; Merényi, R.; Stella, L. *Acc. Chem. Res.* **1985**, *18*, 148.
(22) Kutal, C. *Coord. Chem. Rev.* **1990**, *99*, 213.

Conclusion

1,5-Dimethyl-3-(2′-pyridyl)-6-oxoverdazyl (pvd) is readily synthesized in a manner analogous to the many other verdazyl radicals reported by Neugebauer. EPR spectroscopy suggests that the free radical is very similar to the previously reported 1,5-dimethyl-3-phenyl-6-oxoverdazyl. Like the 3,3′-bis(verdazyl), pvd is a chelating ligand capable of coordinating metal centers. Coordination of group 12 dications results in little perturbation of the singly occupied molecular orbital by EPR and small changes in the UV−vis spectrum suggesting that the ligand is similar to other polypyridyl ligands.

Acknowledgment. This work was supported through the University of Detroit Mercy Faculty Grant Incentive Program (to D.J.R.B.) and the Petroleum Research Foundation (31622-AC to T.H.K.). Facilities for the molecular orbital calculations were provided by the Emerson Center for Scientific Computation. X-ray structure determinations were performed using equipment acquired under National Science Foundation Grant CHE-9505926.

Supporting Information Available: Tables listing detailed crystallographic data, atomic positional parameters, and bond lengths and angles. This material is available free of charge via the Internet at http://pubs.acs.org.

IC9903883